Volume 10, Issue 1, 2020, 4922 - 4928 ISSN 2069-5837
Biointerface Research in Applied Chemistry
www.BiointerfaceResearch.com
https://doi.org/10.33263/BRIAC101.922928
Original Research Article Open Access Journal
Received: 22.10.2019 / Revised: 29.12.2019 / Accepted: 03.01.2020 / Published on-line: 04.01.2020

Sharp changes in properties of aqueous sodium chloride solution at "critical" concentrations of the salt

Elena V. Lasareva [1,*], Aksana M. Parfenova [1], Mikhail K. Beklemishev [1]
[1]Lomonosov Moscow State University, Department of Chemistry, 119991, Moscow, Russia
*corresponding author e-mail address: ***elasareva@ya.ru*** | Scopus ID 26642537300

ABSTRACT
It was shown that some physicochemical properties of aqueous solutions of sodium chloride (contact angle, surface tension, pH, and others) demonstrate a nonlinear dependence on the salt concentration. The maxima or minima in the graphs are most frequently observed near the concentrations of NaCl we call "critical": 3, 5, 7, 12, 17, and 21 g/L. Similar nonlinear peak-shape dependence of the property on salinity was observed in more complex systems containing NaCl (sedimentation rate of mineral suspensions, viscosity of clay pastes, rate of a redox reaction of periodate with amine). We hypothesized that the said critical points of salt concentration may exist when the clusters of water molecules rearrange themselves upon the addition of a definite quantity of salt. The obtained results were used in the discussion of avalanche sedimentation of suspended particulate matter and colloids transported by rivers through the river mixing zones (estuary, delta) and the critical salinity under which the river biota gives place to marine biota.
Keywords:*sodium chloride solutions, critical salinity, water structure, suspended particulate matter, river mixing zone.*

1. INTRODUCTION
Properties of water and aqueous salt solutions play a crucial role in environmental, physiological and various industrial processes. The main component of seawater is sodium chloride that in large measure determines biogeochemistry of the ocean. This substance controls the behavior of riverine matter transport in mixing zones (estuary, delta) [1, 2]. The mixing zone with salinity changing from 3 to 15 g/L is characterized by aggregation and sedimentation of the most part of suspended, colloid and dissolved riverine matter due to the increase of the ionic strength of water [3-7]. The range of 5–8 g/L is the critical salinity for river living organisms when marine biota replaces river biota at increasing salinity and the major biotic and abiotic processes demonstrate non-linear dynamics of change in rates and directions [8-10]. Simulation of flocculation of minerals (clays, carbonate, ferric hydroxide) which are similar to riverine particulate matter and colloids at increasing salt concentrations showed nonlinear behavior of their aggregative stability in the same range of salinity [11-13]. Non-conservative behavior of dissolved organic carbon (DOC), that means an increase in DOC concentrations at low salinity in an estuarine area, was found in some studies [14-16]. These data contradict the traditional approach of conservative behavior of DOC in mixing zones, in which the concentration of DOC decreases due to dilution of river water by sea water. Increased values of DOC in this case were explained by researchers as experimental uncertainty [17, 18].

The studies on physicochemical properties of model and natural solutions containing NaCl showed that there are “critical” points of salinity in which parameters of systems deviate from a linear dependence. It was suggested that such critical points of salinity may appear in the salt solutions when existing clusters of water reformed into new ones involving the salt [19-21]. For example, it was shown that the integral heat of solution at 25°C increased sharply at NaCl concentrations from 0 to 1 g/L and decreased for the concentrations over 5 g/L [22]. Studying macroscopic manifestation of orientational order in the H-bond network of aqueous electrolyte solutions, Chen et al. showed that measured surface tension for NaCl solutions had a sharply defined minimum value at 2 mM. Unfortunately, the surface tension measurements were carried out only at the low concentrations of NaCl [23]. The rheological behavior of sulfomethylated phenolic resin used as a drilling mud additive, changed when the concentration of NaCl reached 0.1 M (5.9 g/L) [24]. The aggregation rate of multiwall carbon nanotubes suspension was not just accelerated at critical NaCl concentrations but also exhibited a peak-shaped relationship versus such concentrations [25]. The effects of salinity on the aggregation of crude oil stabilized by clay particles were determined by Khelifa et al. [26]. It was shown that the median and maximum sizes and the concentration of droplets increased rapidly when salinity of water increased from zero to a critical aggregation salinity in the range of 1.2–3.5 g/L. Non-monotonic dependence of the osmotic virial coefficient of globular protein solutions and their cloud point wasdetermined by computer simulations [27, 28].

It was found that the attractive interaction parameter λ, controlling the variation of the measured protein diffusion coefficient with volume fraction, exhibited a sharp minimum upon an increase of ionic strength of lysozyme solutions [29]. The most efficient relief of nasal congestion gave saline nasal drops containing 9 g/L of NaCl [30]. The maximum degree of aggregation of Newcastle disease virus protein occurred within the concentration of NaCl between 0.7 and 7 mM (0.4–4.1 g/L). Precipitation of proteins under such conditions was used for purification of matrix proteins from other viruses [31]. An interesting approach to the fate of marine biota under increasing salinity was suggested by Khlebovich [8]. His concept of critical salinity postulated a sharp change in abiotic and biotic processes at

a salinity of approximately 5–8 g/L. Further development of such concept in the view of new findings concerning RNA has been expanded to the hypothesis of proto-evolution in which critical salinity was assumed to be the salt concentration level at which the sodium pump emerged in the ancestors of modern animals experiencing an increase of the sodium content in the environment. All those findings showed unusual behavior of system properties at NaCl concentrations below 10 g/L.

To explain such behavior of NaCl solutions it is necessary firstly to refer to water structure that is essentially inhomogeneous. More than a century ago Roentgen pitched an idea of structural heterogeneity of liquid water. The idea was developed in the works of Samoylov [32] (who considered water as ice-like structure), in the clathrate theory by Pauling [33] and a newer model of the water structure (as chains or rings penetrating into the network of disordered clusters with weak H-bonds) [34]. Another recent approach was based on EXAFS spectroscopy study confirmed by X-ray emission spectroscopy; it showed that water has two different structural motifs [35]. According to the new findings, water may be considered as a fluctuating mixture of 1-2-nm clusters of two types, in one of which the molecules are linked as in ice while in the other one the links are disturbed, which leads to a more compact structure [36, 37].

The aim of the present work was to indicate the "critical" points in which the physicochemical properties of NaCl aqueous solutions exhibited nonlinear behavior and to compare them with the data on aggregative stability of particulate matter obtained in the mixing zones of rivers. The results of our study may be of interest tothe understanding of biogeochemical processes in the mixing zones and designing of technological processes (water purification, remediation of saline soils and so on).

2. MATERIALS AND METHODS

2.1. Materials.

Riverine, estuarine and sea water samples were collected during the 54th (September, 2007) and 63th (September, 2015) cruises of research vessel “Academician Keldysh” in the White, Kara and Laptev seas.

Marine and estuarine waters were simulated by the addition of chemically pure sodium chloride (Russian State Standard GOST 4233-77) to distilled water.

To simulate riverine suspended matter we used chemically pure calcite, grain size ~15 μm, and aragonite, synthesized according to Wray and Daniels [38].

3,3’,5,5’-Tetramethylbenzidine (TMB) was purchased from Merck, $MnSO_4$ hydrate was from Sigma–Aldrich, and NaIO4 was from Serva. Distilled water was used to prepare solutions and suspensions.

2.2. Methods.

2.2.1.Drop shape analysis (contact angle).

Drop shape analysis (DSA) as an image analysis method for determining the contact angle from the shadow image of a sessile drop was used. Using a contact angle the surface tension may be calculated using the Young-Laplace equation: $\cos\theta = (\sigma_{sv} - \sigma_{sl})/\sigma_{lv}$, where σ_{sv} is the surface tension on the solid-vapor boundary, σ_{sl} is the surface tension on the solid-liquid boundary, and σ_{lv} is the surface tension on the liquid-vapor boundary. For the determination of a contact angle, a drop of distilled water or salt solutions was metered onto a Teflon plate. An image of the drop was recorded with a photocamera and treated by the drop shape analysis software “Promer”. A contour recognition was initially carried out based on a grey-scale analysis of the image. On the second step, a geometrical model describing the drop shape was fitted to the contour. The contact angle was given by the angle between the calculated drop shape function and the sample surface, the projection of which in the drop image was referred to as the baseline. The accuracy of the method is ±1° [39].

Axioskop 40 Peol microscope (Carl Zeiss, Germany) was used for obtaining the dimensions of particle aggregates.

2.2.2. Maximum bubble pressure method.

Maximum bubble pressure method was used to measure the surface tension of water and salt solutions [40]. In this method a capillary is immersed into the liquid to be measured, and a gas bubble is created inside the liquid using gas with controllable pressure. As the pressure increases, the size of the bubble increases until its diameter is identical to the diameter of the capillary (hemispherical bubble). The pressure at this case is at a maximum and the Young-Laplace equation (above mentioned) allows determining the surface tension. To measure the surface tension we used NaCl solutions with the concentration in the range from 0 to 32 g/L.

2.2.3. The pH measurement.

The pH values of the salt solution were measured using Expert-001 ionomer (Econix-Expert, Russia). The samples of NaCl solutions were studied at 20°C after the dissolution of the weighed quantity of NaCl in the distilled water. All solutions were kept and measured in glassware pretreated with chromic-sulfuric acid mixture.

2.2.4. The study of aggregative stability of calcite and aragonite suspensions.

The weighed quantities of calcite (10 mg each) were placed into a series of 25-mL test tubes with glass stoppers containing 20 mL of distilled water. A known quantity of NaCl was added in each tube so that the concentration of salt changed within 0 to 30 g/L with a step of 0.5 or 1 g/L. The solutions were mixed and left for 15 min at 20°C. Afterwards, an aliquot was taken from the transparent upper layer of liquid and the absorbance was measured at 535 nm using Agilent-8453 spectrophotometer (Agilent Technologies, USA). The experiments with aragonite were conducted in the same way except that the weight of the mineral was 25 mg and the new portions of salt were added to one and the same container between the successive measurements.

2.2.5. Oxidation of 3,3’,5,5’-tetramethylbenzidine with periodate.

The following solutions were mixed in the said order in a glass test-tube: 500 μL of 0.05 $mol \cdot L^{-1}$ sodium acetate (as buffer), 500 μL of 0.1 mg/L Mn^{2+} (as catalyst, taken as sulfate), 125 μL of 0.01 $mol \cdot L^{-1}$ethanolic solution of TMB (color-forming reductant), 3.4 mL of water and 500 μL of freshly prepared $4.3 \cdot 10^{-4}$ $mol \cdot L^{-1}$ solution of $NaIO_4$. The test tube was shaken for about two seconds, the solution was poured into a quartz cell (1×1 cm) and its absorbance measured at 650 nm against water every 30 sec during 6 min [41]. To estimate the influence of salt on the rate of

reaction, the weighed quantity of NaCl was added before the addition of all reagents.

3. RESULTS

3.1. The pH measurement.

For example, the study of pH dependence of NaCl solutions as a function of its concentration showed an extreme value at 6.5 g/L (Fig. 1). It is interesting to mention that the pH equilibration time is longer in the extreme points. Thus, at 6.5 g/L NaCl the equilibrium was only reached in 20 min, as for the other points it was established in several minutes.

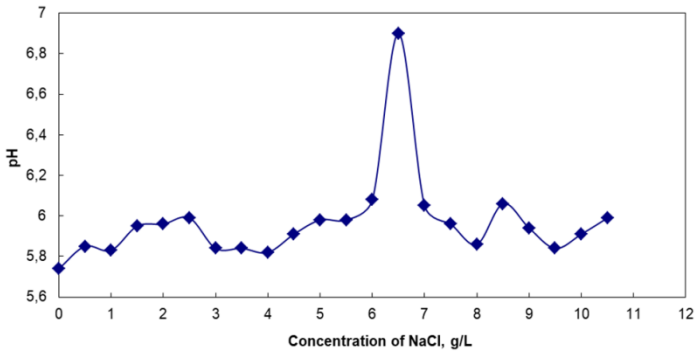

Figure 1. Dependence of pH on the concentration of NaCl solutions in distilled water.

3.2. Measurement of contact angles and surface tension on the water-air boundary.

To confirm the nonlinear behavior in other NaCl solution systems we studied the contact angles (θ) of NaCl aqueous solutions on a Teflon plate. Fig. 2 demonstrates minimal values at 1.5; 3; 7; 12; 15; 17; 22 and 26 g/L (Fig. 2). It is well-known that water has the highest surface tension (σ) among solvents. Surface tension of water slightly increases with the concentration of NaCl. Besides, we observed negative peaks of σ values at 3–4, 12, 17 and 22 g/L (Fig. 3).

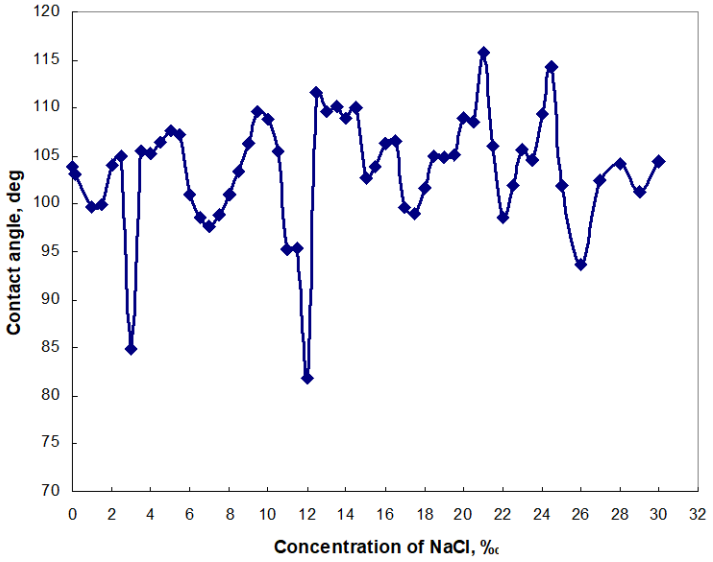

Figure 2. Dependence of the contact angle of NaCl aqueous solutions on a Teflon plate as a function of NaCl concentration.

3.3. Reaction rate of periodate oxidation of 3,3',5,5'-tetramethylbenzidine.

This reaction was catalyzed with Mn(II) at pH around 7 to yield a blue-green product of one-electron oxidation of TMB [41].NaCl affected the rate of the color product accumulation in the way illustrated in Fig. 4. For the reaction times of ≤2 min, the reaction rate was peaking at 2 to 3; 4.8; and 7.5 g/L NaCl. For the times closer to equilibrium (>2 min) the two latter peaks combined into a plateau, and the pattern became less clear.

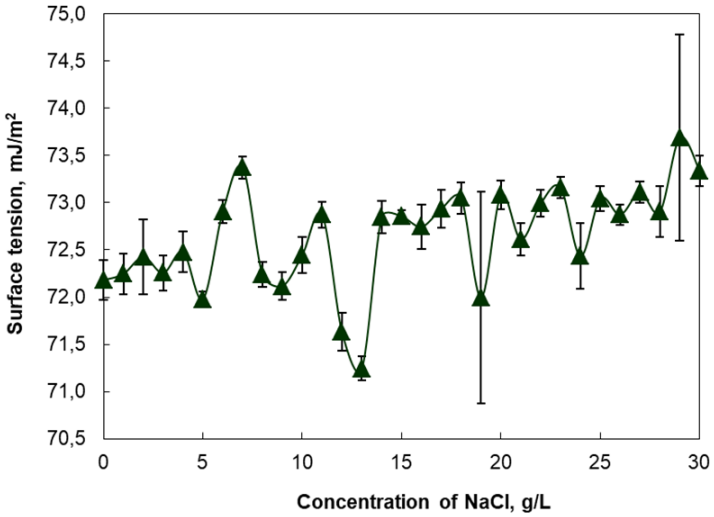

Figure 3. Dependence of the surface tension on sodium chloride concentration (4 parallel runs for each experiment).

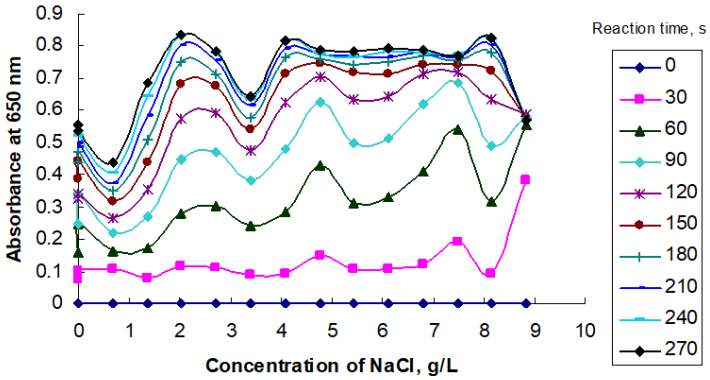

Figure 4. Effect of NaCl concentration on the absorbance of the oxidation product of TMB with periodate for various reaction times (sec) shown in the legend.

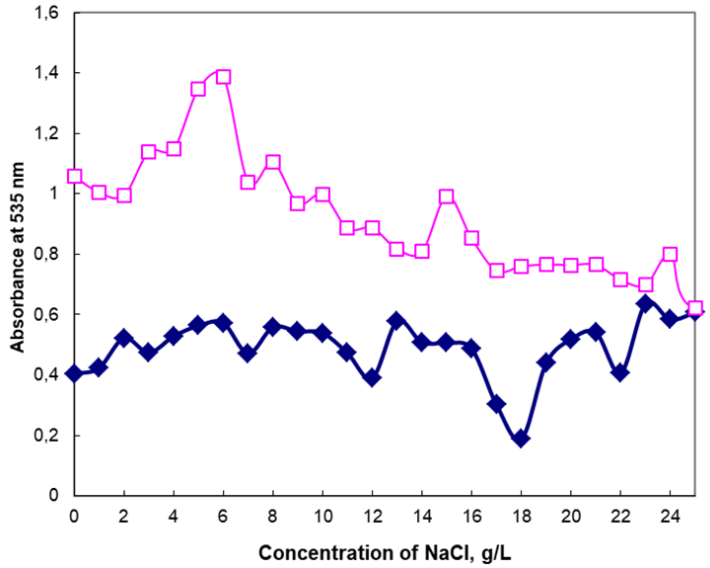

Figure 5. Dependence of the absorbance of aragonite (upper curve) and calcite (lower curve) suspensions on the concentration of NaCl (the portions of salt were sequentially added to one and the same container).

3.4. The aggregative stability of calcite and aragonite suspensions.

The absorbance (as a measure of turbidity) of aragonite suspension was measured after the successive addition of weighed portions of NaCl to the suspension in the same container. We found that the extreme values of turbidity wereobserved at 5–6; 15; and 24 g/L (Fig. 5, upper curve). On the contrary, the absorbance of calcite suspensions (Fig. 5, lower curve) versus salinity showed minima at 3; 7; 12; 17–18 and 22 g/L: the suspension at these NaCl concentrations was less turbid implying maximum flocculation and sedimentation. This finding agrees with our previous experiments with kaolinite suspension in the presence of chitosan [11] that showed minimal absorbance at 7 g/L NaCl.

3.5. Relation of "critical" NaCl concentrations to the river–sea barrier properties.

Salinity is the main environmental factor thatplays a decisive role in transport of riverine runoff in estuaries. The data obtained in the water of the mixing zone of the Northern Dvina River [12, 13, 16] showed that elevated concentrations of particulate suspended matter (PM) were revealed at salinities between 2.9 and 6.4 g/L. Alongside a decreasing concentration of particulate organic carbon (POC) at increasing salinity, elevated concentrations of POC were determined at 2.9, 11.9 and 18.5 g/L. The POC/PM ratio that indicates coagulation and flocculation in the mixing zone shows maxima values at the same concentrations (Table 1).

Table 1. Particulate matter in the surface water layer of the mixing zone of Northern Dvina River (Kochenkova et al., 2018)

S, g/L	PM, mg/L*	POC, mg/L*	POC:PM, %
0.5	4.14	0.34	8.2
1.3	3.89	0.36	9.3
2.9	**4.01**	0.42	**10.5**
6.4	**4.63**	0.32	6.9
8.8	3.45	0.24	7.0
11.9	3.21	0.32	**9.9**
14.5	2.27	0.12	5.3
18.5	1.40	0.20	**14.3**
21.1	1.13	0.12	10.6

*PM is particulate matter; POC is organic carbon of particulate matter.

3.6. Discussion.

Interaction of electrolytes with water occurs in many ways: changing dipole orientation, inducing charge transfer, and distorting the hydrogen-bond network in the bulk and at interfaces. Electrolytes induce orientational order may cause nonspecific changes in some solution properties [23]. In the Introduction we mentioned a large set of literature data on untypical behavior of NaCl solutions at particular concentrations. We believe that these publications would have been even more numerous if the anomalous behavior of salt solutions at certain concentrations had not been regarded as outlayers, and the change in salt concentration had been smaller. Besides, some results might have been remained unpublished due to the lack of interpretation. In our experiments (some of them are summarized in Table 2) we showed that the solution properties near the concentrations of 3, 5, 7, 12, and 17 g/L NaCl had extreme values, which implies extreme deviations from the linear behavior. It is noteworthy that we used the step of concentration of 1.0, 0.5 g/L or even narrower. If this step had been, for instance, 5 g/L, we would not have been able to observe the extreme values. The structure and dynamics of water around ions have been studied by different methods such as X-ray and neutron scattering [42], X-ray absorption spectroscopy [43], Raman spectroscopy [44], and others [23].

Models of pure water structure regard it as a system containing at least two pseudo-phases [36, 37]. In salt solutions of units of permille concentrations, most of water is associated with the ions of the salt (up to three hydration shells around individual ions of electrolytes have been detected) [23]. Therefore, when considering the solutions of salts, it would be natural to conceive that the two pseudo-phases are the (1) strongly bound water of the inner hydration shells and (2) the loosely bound water of the outer hydration shell. Moreover, it may be hypothesized that each hydration shell can contain only a *limited* number of water molecules. Then, dilution of solution is equivalent to adding some weaker bound water to the outer hydration shell. However, water will be joining the outer hydration shell *until it is completed*. When adding more water than the upper hydration layer can accept, the free water will start forming the next, more loose hydration layer, and the macroscopic properties of the solution will change more or less sharply. Further dilution would iterate these events during the formation of the next hydration layers.

Some field observations may illustrate the rearrangement of the “shell” structure of hydrated ions. It is well-known that the salinity gradient determines the fate of riverine runoff, including toxic substances that get to river water. A growing focus on the Artic rivers is primarily inspired by the current and predicted climate change trends that lead to an increase of melting permafrost and consequently to changes in coastal-estuarine ecosystems. It is important to understand the mechanisms of physical-chemical processes occurring to riverine matter when in contact with salt water [45]. It is known that the dominant salt-induced changes occur at salinity 3 - 15 g/L and are connected with coagulation and flocculation of the major riverine matter in the mixing zone [1, 2, 13]. Satellite data in the fluvial–marine transition zone in the Laptev Sea and colored dissolved organic matter fluorescence data of the surface water from estuarine regions of Khatanga, Kolyma and Indigirka rivers in the East Siberian Sea demonstrated rapid removal of dissolved organic carbon (DOC) in coastal waters [46, 47]. It is interesting to mention that the removal of riverine materials had non-monotonous character and maximum fluctuation was found in the mixing zone at critical salinity [12].

Earlier we found that the concentration of dissolved carbohydrates in estuarine waters of the Amazon River had maximum values at salinities 1 and 10 g/L [48]. This non-linearity may be attributed to many factors: seasonal aspect, the variability of composition and fluxes of fresh water over the time-scale comparable to the water residence time in the estuary, or some others [49]. Along with that, the non-linearity may imply the existence of special salinity values at which biogeochemical processes lead to the aggregation of colloids, suspended particulate matter and DOC of riverine runoff in the mixing zone. The decrease of their concentrations in water as well as the concentrations of polluting substances (metals, oil) that may coprecipitate with the formed aggregates may be connected with the biological processes taking place at the critical gradient. Biological species undergo osmotic stress at critical salinity and

release soluble organic substances due to osmotic lysis or viral shunt. This newly formed DOM may contribute to the aggregation process, leading to the flocculation of suspended matter [10, 13, 50].

It is also necessary to mention that the "critical points" of water may vary for different aqueous systems. This can happen because water is a flexible system responding to the Earth's magnetic field, radiation, and other environmental factors [51]. The purpose of this study was not to collect large statistics, but rather to attract attention to the fact of periodic change of physico-chemical characteristics of water solutions versus NaCl concentration. We believe that this information may be interesting for chemists, members of the medical professions, physicists and biologists who deal with salt solutions (virtually all natural solutions contain electrolytes). One such system is a riverine mixing zone in which most important biogeochemical processes of inanimate and living matter transformation happen inthe area of intermediate salinity values.

Table 2. Concentrations of NaCl at which extremal values of the parameters were observed

Parameter	Critical concentrations, g/L				
Contact angle	3	6	–	11–12	Not studied
Viscosity	–	5–6	–	10	Not studied
Reaction rate*	3.5	5	7.5; (9)	Not studied	Not studied
Surface tension	–	6–7	–	12–13	–
pH (equilibrium)	–	6.5	–	–	–
POC:PM, %**	3	–	–	12	18.5

* Oxidation of 3,3',5,5'-tetramethylbenzidine with perodate

** Organic carbon of particulate matter to suspended matter ratio (see Table 1)

4. CONCLUSIONS

Based on literature and own data, we have shown the existence of several "critical" points of peak-shape behavior of aqueous solutions and suspensions with increasing NaCl concentration. Hypothetically, these "critical" concentrations of the salt are connected to the proportion of water containing in the hydration shells of the ions and "free" water. The observed critical phenomena, associated with the reformation of the water structure with increasing salinity, may affect the riverine matter transport in the mixing zones and explain the existence of specific salinity values invoking the most intense coagulation and flocculation of riverine particulate, dissolved and colloid matter.

5. REFERENCES

1. Lisitzin, A.P. The continental-ocean boundary as a marginal filter in the World Oceans. In *Biogeochemical Cycling and Sediment Ecology*. Gray, J.S., Ambrose, W., Szaniawska, A., Eds.; NATO ASI Series (Series E: Applied Sciences), vol 59. Springer, Dordrecht, 1999; pp. 69-109, https://doi.org/10.1007/978-94-011-4649-4_4.
2. Johnston, S. E.; Shorina, N.; Bulygina, E.; Vorobjeva, T.; Chupakova, A.; Klimov, S. I, et al. Flux and seasonality of dissolved organic matter from the Northern Dvina (Severnaya Dvina) River, Russia. *Journal of Geophysical Research: Biogeosciences* 2018, 123, https://doi.org/10.1002/2017JG004337.
3. Pokrovsky, O.S; Shirokova, L.S.; Viers, J.; Gordeev, V.V.; Shevchenko, V.P.; Chupakov, A.V. Dissolved organic carbon and organo-mineral colloids in the mixing zone of the largest European Arctic River. In:*Dissolved organic matter (DOM): properties, applications and behavior*. Pokrovsky, O.S., Shirokova, L.S. Eds.; Nova Science Publ, Inc, New York, USA, 2017; pp. 273–291.
4. Sholkovitz, E.R. Flocculation of dissolved organic and inorganic matter during the mixing of river water and seawater. Geochim. *Cosmochim. Acta* **1976**, *40,* 831-845,https://doi.org/10.1016/0016-7037(76)90035-1.
5. Sholkovitz, E.R.; Boyle, E.A.; Price, N.B. The removal of dissolved humic acids and iron during estuarine mixing. *Earth Planet Sci. Lett.* **1978**, 40, 1, 130-136. https://doi.org/10.1016/0012-821X(78)90082-1.
6. Lee, B.J.; Hur, J.; Toorman, E.A. Seasonal Variation in Flocculation Potential of River Water: Roles of the Organic Matter Pool. *Water* **2017**, *9*, 335, https://doi.org/10.3390/w9050335.
7. Tan, X.L.; Zhang, G.P.; Yin, H.; Reed, A.H.; Furukawa, Y. Characterization of particle size and settling velocity of cohesive sediments affected by a neutral exopolymer. *Int J Sediment Res*. **2012**, *27,* 473-485, https://doi.org/10.1016/S1001-6279(13)60006-2.
8. Khlebovich, V.V. Critical salinity as a marker of transition from the potassium era of life development to the sodium era. *Biol. Bull. Rev.* **2015,** *5,* 308-310, https://doi.org/10.1134/s2079086415040039.
9. Khlebovich, V.V. *Critical Salinity of Biological Processes.*Nauka, Leningrad, Russia, 1974; pp. 236.
10. Telesh, I.V.; Khlebovich, V.V. Principal processes within the estuarine salinity gradient: A review. *Marine Pollution Bull.* **2010**, *61,* 149–155, https://doi.org/10.1016/j.marpolbul.2010.02.008.
11. Lasareva, E.V.; Romankevich, E.A. Transport of organic matter and clay minerals in estuaries of Arctic sea (Experimental and Field Observations). *Oceanol. Marine Chem*. **2009**, *49*, 47-54, https://doi.org/10.1134/S0001437009010068.
12. Lasareva, E.V.; Parfenova, A.M.; Demina, T.S.; Romanova, N.D.; Belyaev, N.A.; Romankevich, E.A. Transport of the colloid matter of riverine runoff through estuaries. *Oceanol. Marine Chem.* **2017**, *57,*520–529, https://doi.org/10.1134/S0001437017040130.
13. Lasareva, E.V.; Parfenova, A.M.; Romankevich, E.A.; Lobus, N.V; Drozdova, A.N. Organic matter and mineral interactions modulate flocculation across Arctic river mixing zones. *Journal of Geophysical Research: Biogeosciences* **2019**, *124,* 1-14, https://doi.org/10.1029/2019JG005026.
14. Raymond, P.A.; Spencer, R.G.M. Riverine DOM. In:*Biogeochemistry of Marine Dissolved Organic Matter*. 2nd ed., Hansell, D.A., Carlson, C. A. Eds., Elsevier, Amsterdam, **2015**, pp. 509–533, https://doi.org/10.1016/b978-0-12-405940-5.00011-x.
15. Gonçalves-Araujo, R.; Stedmon, C.A.; Heim, B.; Dubinenkov, I.; Kraberg, A.; Moiseev D.; Bracher, A. From fresh to marine waters: characterization and fate of dissolved

organic matter in the Lena River Delta region, Siberia. *Front. Mar. Sci.* **2015,** *108,* 1-13, https://doi.org/10.3389/fmars.2015.00108.
16. Kochenkova, A.I.; Novigatskiy, A.N.; Gordeev, V.V. The distribution of suspended matter in the marginal filter of the Northern Dvina River at the end of the summer. *Adv. Curr. Nat. Sci.***2018**, *2*, 106-112, https://doi.org/10.17513/use.36680.
17. Stein C.R.; Macdonald, R.W.; Naidu, A.S.; Yunker, M.B.; Gobeil, C.; Cooper L.W. et al. Organic carbon in Arctic Ocean Sediments: Sources, Variability, Burial, and Paleoenvironmental Significance. In:*The Organic Carbon Cycle in the Arctic Ocean* Stein, R., Macdonald, R.W. Eds., Springer-Verlag: Berlin, 2004; pp. 169-314, https://doi.org/10.1007/978-3-642-18912-8_7.
18. Pokrovsky, O.S.; Shirokova, L.S.; Viers, J.; Gordeev, V.V.; Shevchenko, V.P.; Chupakov, A.V.; Vorobieva, T.Y.; Candaudap, F.; Causserand, C.; Lanzanova, A.; Zouiten, C. Fate of colloids during estuarine mixing in the Arctic. *Ocean Sci.* **2014**, *10*, 107–125, https://doi.org/10.5194/os-10-107-2014.
19. Sceats, M.G.; Rice, S.A. The water–water pair potential near the hydrogen bonded equilibrium configuration. *J. Chem. Phys.* **1980***, 72,* 3236-3247, https://doi.org/10.1063/1.439560.
20. Speedy, R.J. Self-replicating structures in water. *J. Phys. Chem.* **1984**, *88*, 3364-3373, https://doi.org/10.1021/j150659a046.
21. Malenkov, G.G. Computer Simulations of Structure and Dynamics of Atomic and Molecular Systems. In:Modern Problems in Physical Chemistry.Granitsa: Moscow, 2005; pp. 119–136 [in Russian].
22. Mishchenko, K.P.; Ravdel, A.A. A short reference book on physical and chemical quantities. Eds., Chimiya: Leningrad, Russia, 1974; pp. 200.
23. Chen, Y.; Okur, H.; Gomopoulos, N.; Macias-Romero, C.; Cremer, P.; Petersen, P.; Tocci, G.; Wilkins, D.; Liang, Ch.; Ceriotti, M.; Roke, S. Electrolytes induce long-range orientational order and free energy changes in the H-bond network of bulk water. *Sci. Adv.* **2016**, *2*, e1501891, https://doi.org/10.1126/sciadv.1501891.
24. Zhuang, Y.; Zhu, Z.; Chao, H.; Yang, B. Effect of Added Salt on Properties of Aqueous SMP Solution. *J. Appl. Polym. Sci.* **1995**, *55,*1063–1067, https://doi.org/10.1002/app.1995.070550709.
25. Ntim, S.A.; Sae-Khow, O.; Desai, C.; Witzmann, F. A.; Mitra, S. Size dependent aqueous dispersibility of carboxylated multiwall carbon nanotubes. *J. Environ. Monit.* **2012**, *14,* 2772–2779, https://doi.org/10.1039/c2em30405h.
26. Khelifa, A.; Hill, P.S.; Stoffyn-Egli, P.; Lee, K. Effects of Salinity and Clay Composition on Oil-Clay Aggregations. *Marine Environ. Res.* **2005***, 59,*235-254, http://dx.doi.org/10.1016/j.marenvres.2004.05.003.
27. Allahyarov, E.; Löwen, H.; Hansen, J.P.; Louis, A.A. Non-monotonic variation with salt concentration of the second virial coefficient in protein solutions. *Phys. Rev. E* **2003**, *67,* https://doi.org/10.1103/PhysRevE.67.051404.
28. Wu, J.Z.; Bratko, D.; Blanch, H.W.; Prausnitz, J.M. Monte Carlo simulation for the potential of mean force between ionic colloids in solutions of asymmetric salts. *J. Chem. Phys.* **1999**, *111*, 7084-7094, https://doi.org/10.1063/1.480000.
29. Grigsby, J.J.; Blanch, H.W.; Prausnitz, J.M. Diffusivities of Lysozyme in Aqueous MgCl2 Solutions from Dynamic Light Scattering Data: Effect of Protein and Salt Concentrations. *J. Phys. Chem. B* **2000** *104,* 3645-3650, https://doi.org/10.1021/jp993177s.
30. Principi, N.; Esposito, S. Nasal Irrigation: An Imprecisely Defined Medical Procedure. *Int. J. Environ. Res. and Public Health* **2017**, *14*, 516, https://doi.org/10.3390/ijerph14050516.
31. Sagrera, A.; Cobaleda, C.; Berger, S.; Marcos, M.J.; Shnyrov, V.; Villar E. Study of the influence of salt concentration on Newcastle disease virus matrix protein aggregation. *Biochem. Mol. Biol. Int.* **1998**, *46*, 429-435, https://doi.org/10.1080/15216549800203952.
32. Samoylov, O.Y. Peculiar features of water structure. *J. Struct. Chem*. **1965**, *5*, 6-8.
33. Pauling, L. *The of the Chemical Bond*. 3ed ed., Cornell University Press: Ithaca, New York, 1960; pp. 472.
34. Ludwig, R. *Water: from clusters to the bulk*. Angew. Chem. Int. Ed.: 40, 2001; pp. 1808-1827.
35. Zakharov, S.D.; Mosyagina, I.V. Cluster structure of water. *Preprint of Lebedev Phys. Inst. Russ* **2011**, 1-34.
36. Tokushima, T.; Harada, Y.; Takahashi, O.; Senba, Y.; Ohashi, H.; Pettersson, L.G.M.; Nilsson, A.; and Shin, S. High resolution X-ray emission spectroscopy of liquid water: The observation of two structural motifs. *Chem. Phys. Lett.* **2008**, *460*, 4-6, 387–400, https://doi.org/10.1016/j.cplett.2008.04.077.
37. Huang, C.; Wikfeldt, K.T.; Tokushima, T.; Nordlund, D.; Harada, Y.; Bergmann, U.; Niebuhr, M.; Weiss, T.M.; Horikawa, Y.; Leetmaa, M.; Ljungberg, M.P.; Takahashi, O.; Lenz, A.; Ojamae, L.; Lyubartsev, A.P.; Shin, S.; Pettersson, L.G.M.; Nilsson, A. The inhomogeneous structure of water at ambient conditions. *Proc. Natl. Acad. Sci. USA* **2009**, *106*, 15214–15218, https://doi.org/10.1073/pnas.0904743106.
38. Wray, J.L.; Daniels, F. Precipitation of calcite and aragonite. *J. Am. Chem. Soc.* **1957**, *79*, 2031-2034, https://doi.org/10.1021/ja01566a001.
39. *Practical Manual on Colloid Chemistry for Higher Education Students*.Kulichikhin, V.G. Ed., VuzovskiiUchebnik: Moscow, Russia, **2012**; pp. 94-97. ISBN 9785955802176.
40. Adamson, A.W; Gast, A.P. Experimental methods and measurements of contact angle. In:*Physical Chemistry of Surfaces*. 6th ed.; J. Wiley & Sons Inc.: New York, **1997**; pp. 17-19.
41. Efremova, T.A.; Beklemishev, M.K.; Shumskii, A.N.; Dolmanova, I.F. Catalytic determination of manganese(II) using oxidation of 3,3',5,5'-tetramethylbenzidine by potassium periodate. *Moscow Univ. Chem. Bull. Ser.2, Chem*, **1998**, 39, 4, 261–264.
42. Bouazizi, S.; Nasr, S.; Jaîdane, N.-E.; Bellissent-Funel, M.C. Local order in aqueous NaCl solutions and pure water: X-ray scattering and molecular dynamics simulations study. *J. Phys. Chem.* **2006,** *110,* 46, 23515–23523, https://doi.org/10.1021/jp0641583.
43. Waluyo, I.; Nordlund, D.; Bergmann, U.; Schlesinger, D.; Pettersson, L.G.M.; Nilsson, A. A different view of structure-making and structure-breaking in alkali halide aqueous solutions through x-ray absorption spectroscopy. *J. Chem. Phys.* **2014**, *140*, 244506, https://doi.org/10.1063/1.4881600.
44. Smith J.D.; Saykally, R.J.; Geissler, P.L. The effects of dissolved halide anions on hydrogen bonding in liquid water. *J. Am. Chem. Soc.* **2007**, *129*, 13847–13856, https://doi.org/10.1021/ja071933z.
45. Novigatsky, A.N.; Klyuvitkin, A.A.; Lisitsyn, A.P. Vertical fluxes of dispersed sedimentary matter, absolute masses of the bottom sediments, and rates of modern sedimentation. In: *Sedimentation processes in the White Sea: the White Sea environment, part II, The handbook of environmental chemistry*Lisitsyn, A.P., Demina, L.L. Eds., Volume 82, 2, Springer: Berlin, **2018**; https://doi.org/10.1007/698_2018_278.
46. Juhls, B.; Overduin, P.P.; Hölemann, J.; Hieronymi, M.; Matsuoka, A.; Heim B.; Fischer, J. Dissolved organic matter at the fluvial–marine transition in the Laptev Sea using in situ data and ocean colour remote sensing. *Biogeosciences* **2019**, *16*, 2693-2713,https://doi.org/10.5194/bg-16-2693-2019.

47. Drozdova, A.N., Krylov, I.N.;Shchuka, S.A. CDOM fluorescence of the Laptev Sea and East Siberian surface water. EARSeLe Proceedings **2018**, *17*. https://doi.org/10.12760/01-2018-1-01.
48. Lazareva, E.V.; Romankevich, E.A. Carbohydrates as indicators of biogeochemical processes. *Oceanol. Marine Chem.* **2012**, *52,* 335-344, https://doi.org/10.1134/S0001437012020075.
49. Wetzel, R.G. Limnology: Lake and River Ecosystems. 3rd ed., Academic Press: New-York, **2001**; pp. 1006. eBook ISBN: 9780080574394
50. Dixon, C.; Wilken, L.R. Green microalgae biomolecule separations and recovery. *Bioresour. Bioprocess*. **2018** *5*, https://doi.org/10.1186/s40643-018-0199-3.
51. Ntim, S.A.; Sae-Khow; O., Desai, C.; Witzmann, F.A.; Mitra, S. Size dependent aqueous dispersibility of carboxylated multiwall carbon nanotubes. *J. Environ. Monit*. **2012**, *14,* 2772–2779, https://doi.org/10.1039/c2em30405h.

6. ACKNOWLEDGEMENTS

The authors thank Prof. E.A. Romankevich, the Head of the Laboratory of Ocean Chemistry, P.P. Shirshov Institute of Oceanology of Russian Academy of Sciences, for his great interest to this investigation. The work was supported by the grant RFNP (project № AAAA-A16-116030250108-3).